TOPOLOGY OPTIMIZATION OF A CAR BODY WITH MULTIPLE LOADING CONDITIONS

Junichi Fukushima*
Toyota Technical Center U.S.A., Inc., Southfield, MI

Katsuyuki Suzuki**
The University of Tokyo , Tokyo, Japan

Noboru Kikuchi***
The University of Michigan, Ann Arbor, MI

Abstract

In various practical structural design problems, decision of a layout of structure or stiffeners in the given design space satisfying some design requirements is the most difficult task for design engineers. Since they must consider many possible conditions for safety, performance and so on. It is also very difficult to solve the layout (topology) problem by any conventional structural optimization techniques because its mathematical modeling of topology is so complex. To solve the problem, we employed the new topology/layout optimization technique based on the homogenization method introduced by Bendsøe and Kikuchi. This method gives the minimum compliance design under a certain material constraint.

In this paper we shall study a class of multi-loading problems for topology optimization by the homogenization method, and several car body design problems are solved to justify the validity and the strength of the present method for engineering applications.

1. Introduction

A new type of approach for shape and topology optimization based on the homogenization method was introduced by Bendsøe and Kikuchi [1] and followed by Suzuki and Kikuchi [2] and Suzuki [3]. While conventional shape optimization technique can handle only boundary shape, the new approach can represent arbitrary topology as well as shape just by displaying the gray scale representation of the density of void/solid computed by the present method with supplying a design domain, loading and support conditions, and the amount of materials, as shown in Figure 1. It has great advantage from designer's point of view over conventional methods that the new method does not require any initial topology and shape to be defined as spline functions before optimization.

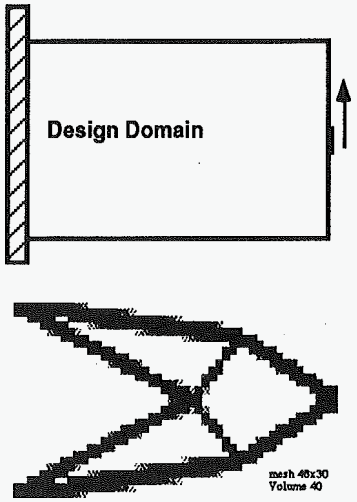

Figure 1. Problem definition and the solution by the homogenization method

In most of the previous work, only one loading condition is considered. But in engineering applications it is necessary to consider several loading conditions as well as support conditions.

---

* Senior Engineer, Technical Research Dept. Member AIAA

** Research Associate, Department of Naval Architecture and Ocean Engineering

*** Professor, Department of Mechanical Engineering and Applied Mechanics

2. Problem and Formulation

2.1 Shape and Topology Optimization Based on The Homogenization Method

The main idea of topology optimization is that infmitely many microscale voids (holes) are introduced to form a porous perforated medium that yields a structure, and the homogenization method was used to determine the averaged elasticity tensor of the perforated medium of rectangular microscopic holes. If the neighborhood of a point is identified with voids, structure is not placed there. On the other hand, if no void exists over there, solid structure is formed.

If porosity does not reach the limit values, porous perforated medium is placed there, see Figure 2. An optimization problem for the shape and topology is defined by solving the optimal porosity of the medium over a design domain specified. The mean compliance is used as the objective function, and the upper limit is given on the total amount of material to form a perforated composite. This optimal void/material distribution problem for a single load case can be written as

$$\underset{\text{perforation}}{Minimize} \quad \sum_{i=1}^{N}\int_{\Omega}\rho f_i u_i d\Omega + \sum_{i=1}^{N}\int_{\Gamma_T} t_i u_i d\Gamma \qquad (1)$$

subject to

Equilibrium Equations

$$\int_{\Omega}\rho(x)d\Omega \le \overline{\Omega} \qquad (2)$$

where N indicates the dimension of the space in which a structure is placed, $\boldsymbol{f}$ and $\boldsymbol{t}$ are the applied body forces in the design domain Ω and tractions on a portion of the specified boundary Γ_t, respectively. ρ is the mass density of the porous perforated structure, and $\boldsymbol{u}$ is the solution of the equilibrium equations

$$\boldsymbol{u} \in V_D \ : \ \sum_{i,j,k,l=1}^{N}\int_{\Omega} E^G_{ijkl}(x)\frac{\partial u_k}{ax,}\frac{\partial v_i}{\partial x_j}d\Omega - \sum_{i=1}^{N}\int_{\Omega} f_i v_i d\Omega + \sum_{i=1}^{N}\int_{\Gamma_T} t_i v_i d\Gamma \quad \forall \boldsymbol{v} \in V_0 \qquad (3)$$

The elasticity tensor $\boldsymbol{E^G}$ homogenized and optimally rotated is a function of the sizes of the rectangular holes, and the angle of rotation θ. The design variables are the distribution of two sizes of holes and a rotational angle. These distributed functions are discretized using the finite element method.

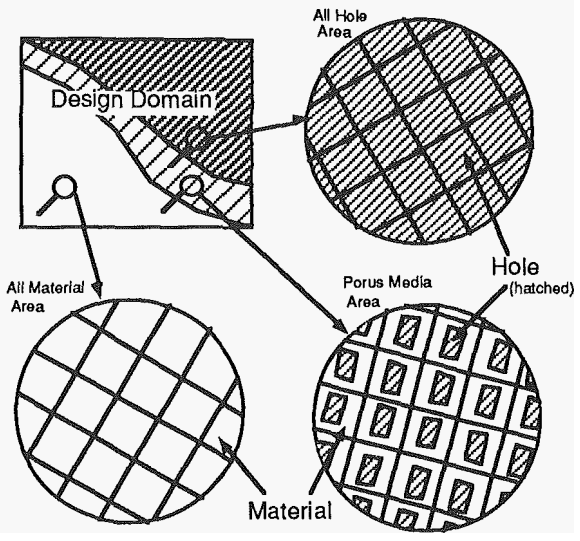

Figure 2. Optimal Distribution of Microstructure

2.2 Multiple Load Problem

Let us extend this formulation for multiple loading conditions. The problem can be interpreted as a multi-objective problem in which there are several objective functions to be minimized or maximized. There are several approaches for the multi-objective problem. The most typical approach is to use some linear combination of the objective functions such as modified global criteria approach [4]. Another typical approach, the ß-method is defined by introducing an additional design variable that is the upper bound of all the objective functions [5]. There are also other effective approaches such as the K-S function approach [6]. Here, we shall use the maximum of the density of the compliance of multiple loadings as the objective function. In other words, we shall minimize the worst objective function. This approach may provide the safest design from the designer's point of view. Mathematically, this is defined by using the new objective function defined by

$$F(\boldsymbol{u}) = \underset{\text{load case } \mathbf{p}}{Maximize} \quad \sum_{i=1}^{N}\int_{\Omega}\rho f_{ip} u_{ip} d\Omega + \sum_{i=1}^{N}\int_{\Gamma_T} t_{ip} u_{ip} d\Gamma \qquad (4)$$

And optimization problem can be defined as

$$\underset{\text{perforation}}{Minimize}\ F(u) \tag{5}$$

subject to

Equilibrium equations for each load and support

$$\int_\Omega \rho(x)d\Omega \le \overline{\Omega} \tag{6}$$

The difficulty of this formulation is that the function $F(u)$ is not necessarily smooth, and then minimizing $F(u)$ may yield non-smooth optimization problem in which differentiability of a function does not hold in some points in the feasible space of the design variables. This non-smoothness often requires very delicate handling, since most optimization techniques assume computation of the sensitivity of the objective function.

2.3 Formulation for the Multiple Load Condition

A method frequently used to avoid a non-smoothness of the objective function is the upper bound approach that introduces a dummy variable β such that

$$\underset{\text{perforation}}{Minimize}\ \beta \tag{7}$$

subject to

$$\beta - \sum_{i=1}^{N}\int_\Omega \rho f_{ip}\, u_{ip} d\Omega - \sum_{i=1}^{N}\int_{\Gamma_T} t_{ip} u_{ip} d\Gamma \ge 0$$

for all load cases p **(8)**

Equilibrium equations for each load and support

$$\int_\Omega \rho(x)d\Omega \le \overline{\Omega} \tag{9}$$

Now that objective function β is differentiable with respect to all design variables. The Kuhn-Tucker conditions are derived using the following Lagrangian.

$$L(a,\theta,u,v,p,q,\Lambda_v) = \beta - \sum_p q_p\left(\beta - \sum_{i=1}^{N}\int_\Omega \rho f_{ip}\, u_{ip}\, d\Omega - \sum_{i=1}^{N}\int_{\Gamma_T} t_{ip}\, u_{ip}\, d\Gamma\right) + \sum_p \Pi(a,\theta,u_p,v_p) + \Lambda_v\left(\int_\Omega \rho\, d\Omega - \overline{\Omega}\right) \tag{10}$$

where,

$$\Pi(a,\theta,u_p,v_p) = \sum_{i,j,m,n=1}^{N}\int_\Omega E^G_{ijmn}(a,\theta)\frac{\partial u_{ip}}{\partial x_j}\frac{\partial v_{mp}}{\partial x_n} d\Omega + \sum_{i=1}^{N}\int_{\Gamma_D}\lambda(u_{ip}-g_i)v_{ip}d\Gamma - \sum_{i=1}^{N}\int_\Omega f_{ip}v_{ip}\, d\Omega - \sum_{i=1}^{N}\int_{\Gamma_T} t_{ip}v_{ip}\, d\Gamma \tag{11}$$

Here, the vector a represents $\{a_1, \ldots, a_N\}$. The Kuhn-Tucker conditions are

$$\frac{\partial L}{\partial a_i}\delta a_i = 0\ ,\ \frac{\partial L}{\partial \theta}\delta\theta = 0$$

for all $\delta a_i = a_i^* - a,\ ,\delta\theta = \theta^* - \mathrm{e}$,

$a_i^*, a_i, \theta^*, \theta \in H^1(\Omega)\ ,\quad 0 \le a_i^*, a_i \le 1$

$$\frac{\partial L}{\partial u_p}\delta u_p = 0,\quad \frac{\partial L}{\partial v_p}\delta v_p = 0 \text{ for each load casep}$$

$$\frac{\partial L}{\partial \beta} = 0$$

$$q_p\left(\beta - \sum_{i=1}^{N}\int_\Omega \rho f_{ip}u_{ip}d\Omega - \sum_{i=1}^{N}\int_{\Gamma_T} t_{ip}u_{ip}d\Gamma\right) = 0,$$

$$q_p \ge 0,\ \beta - \sum_{i=1}^{N}\int_\Omega \rho f_{ip}u_{ip}d\Omega - \sum_{i=1}^{N}\int_{\Gamma_T} t_{ip}u_{ip}d\Gamma \ge 0 \quad \text{for each } p$$

$$\Lambda_V\left(\int_\Omega \rho\, d\Omega - \overline{\Omega}\right) = 0,\quad \Lambda_V \ge 0,\quad \int_\Omega \rho\, d\Omega - \overline{\Omega} \le 0 \tag{12}$$

Although these formulations are mathematically reasonable, it is hard to make an algorithm of the optimality criteria method that yields a resizing rule, since there are too many constraints and hence too many optimality criteria to be satisfied.

In order to overcome this difficulty, another approach is introduced by modifying the objective function shown by **(4)** and by using another objective function that is smooth. Noting that v_{ip} satisfies equilibrium equations of each load case, and then

$$\sum_{i,j,k,l=1}^{N}\int_\Omega E^G_{ijkl}(a,\theta)\frac{\partial v_{kp}}{\partial x_l}\frac{\partial v_{ip}}{\partial x_j}d\Omega = \sum_{i=1}^{N}\int_\Omega f_{ip}v_{ip}d\Omega + \sum_{i=1}^{N}\int_{\Gamma_T} t_{ip}v_{ip}d\Gamma \tag{13}$$

if all the displacement boundary conditions are specified as zero. Hence our problem **(4)** - (6) can be written as

$$\underset{\text{perforation}}{Minimize}\quad \underset{\text{load case p}}{Maximize}\quad \sum_{i,j,k,l=1}^{N}\int_{\Omega} E^{G}_{ijkl}(a,\theta)\frac{\partial v_{kp}}{\partial x_l}\frac{\partial v_{ip}}{\partial x_j}d\Omega \tag{14}$$

subject to

Equilibrium equations of each load

$$\int_{\Omega}\rho(a)d\Omega \le \overline{\Omega} \tag{15}$$

We may use the internal energy as an objective function instead of the external work. Since **(13)** yields the mean compliance of each is the same to twice of the strain energy, we shall introduce the function

$$\overline{F}(u)=\int_{\Omega}\left\{\underset{\text{load case p}}{Maximize}\ \sum_{i,j,k,l=1}^{N} E^{G}_{ijkl}(a,\theta)\frac{\partial v_{kp}}{\partial x_l}\frac{\partial v_{ip}}{\partial x_j}\right\}d\Omega \tag{16}$$

defined by the maximum strain energy density of all the loads of the multiple load problem, and then we shall introduce an approximation of the problem {(14),(15)}:

$$\underset{\text{perforation}}{Minimize}\ \overline{F}(u)$$

subject to

Equilibrium equations of each load

$$\int_{\Omega}\rho(a)d\Omega \le \overline{\Omega} \tag{17}$$

It should be noted that this new problem is not equivalent to the original one, but we have the following relation:

$$\underset{\text{load case p}}{Maximize}\ \sum_{i,j,k,l=1}^{N}\int_{\Omega} E^{G}_{ijkl}(a,\theta)\frac{\partial v_{kp}}{\partial x_l}\frac{\partial v_{ip}}{\partial x_j}d\Omega \le \int_{\Omega}\underset{\text{load case p}}{Maximize}\left\{\sum_{i,j,k,l=1}^{N} E^{G}_{ijkl}(a,\theta)\frac{\partial v_{kp}}{\partial x_l}\frac{\partial v_{ip}}{\partial x_j}\right\}d\Omega \tag{18}$$

Hence

$$\underset{\text{perforation}}{Minimize}\quad \underset{\text{load case p}}{Maximize}\quad \sum_{i,j,k,l=1}^{N}\int_{\Omega} E^{G}_{ijkl}(a,\theta)\frac{\partial v_{kp}}{\partial x_l}\frac{\partial v_{ip}}{\partial x_j}d\Omega \le \underset{\text{perforation}}{Minimize}\int_{\Omega}\underset{\text{load case p}}{Maximize}\left\{\sum_{i,j,k,l=1}^{N} E^{G}_{ijkl}(a,\theta)\frac{\partial v_{kp}}{\partial x_l}\frac{\partial v_{ip}}{\partial x_j}\right\}d\Omega \tag{19}$$

For numerical solution technique, the sensitivity of the load case which gives the maximum value of strain energy density for each point in design domain is used in the update rule of sizes of holes, and the principal stress direction of the same load case is used in determining the rotational angles of microstructure.

3. Three-Bar Frame Structure Comparison of Two Objective Function

3.1 Problem Definition

Three bars are placed as shown in Figure 2: two bars are placed with **45** degree to the ceiling symmetrically, and a bar is vertical to the ceiling. Three loadings shown in Table **1** are applied. For this calculation circular cross section beam elements with bending and shear stiffness are used. This problem was first solved by Sheu and Schmit [7] as the three bar truss problem.

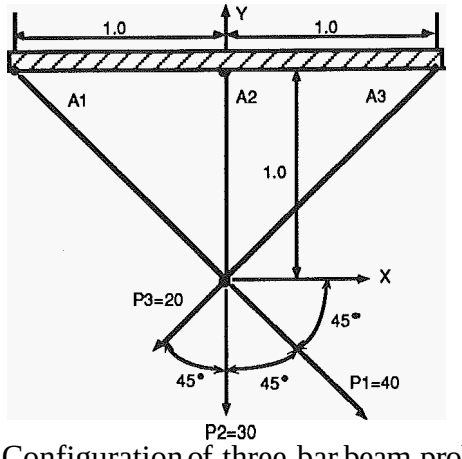

Figure 2 Configuration of three-bar beam problem

Table **1** Loading Conditions

Load Case	F_x	F_y
1	-14.14	-14.14
2	0	-30
3	28.28	-28.28

3.2 *MP* Solution with the Original Formulation

The problem with original formulation by (7),(8) and (9) is solved using mathematical programming method [8]. Design variables are cross sectional areas of each element. The upper limit of the volume was set to 10.0. Table 2 shows the initial and final values of design variables, the objective functions and the volume of the structure.

Table 2 Mathematical Programming Solution with the Original Problem Formulation

	Initial	Final
A1	1.0	6.22
A2	1.0	1.23
A3	1.0	0.0
Objective	1320.4	320.2
Volume	3.828	10.0

3.3 MP Solution with a Modified Formulation

We solved the same problem using modified objective function which is the summation of maximum of all load cases in each element defined by equation (16). Table 3-A is the final values of design variables, objective function and volume of the model. In Table 3-B compliances of each element in each load are listed.

Table 3-A Mathematical Programming Solution with a Modified Problem Formulation

	Initial	Final
A1	1.0	3.87
A2	1.0	4.57
A3	1.0	1.8E-8
Objective	1362.1	346.9
Volume	3.828	10.0

Table 3-B Final Compliance Values

Element ID	Loadcase 1	Loadcase 2	Loadcase 3
1	41.29	26.62	217.31
2	104.62	129.61	129.62
3	6.8E-7	3.5E-7	2.8E-7

3.4 Comparison of Two Objective Functions

From the results of three-bar example, we can find that the modification of the objective function like (17) is quite reasonable to simplify the multi-objective problem. The objective function by (10) is **8.3%** higher than the one for the original problem, while the final size of the bars is not *so* close despite that the topology of the optimum structure is the samw. Figure 3-A and Figure 3-B are contour plots of two objective functions of several sections of two of design variables. Basically, both objective functions have the same characteristics. This means the modification of the objective function may not affect too much to the optimum obtained by numerical computation. It is, however, noted that the approximation in (17) does not yield the minimum. In other words, the design by the approximation (17) results just a suboptimum solution.

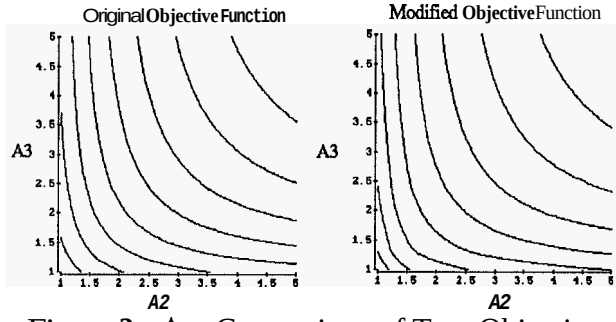

Figure 3 - A Comparison of Two Objective Functions (A1 = 1.0)

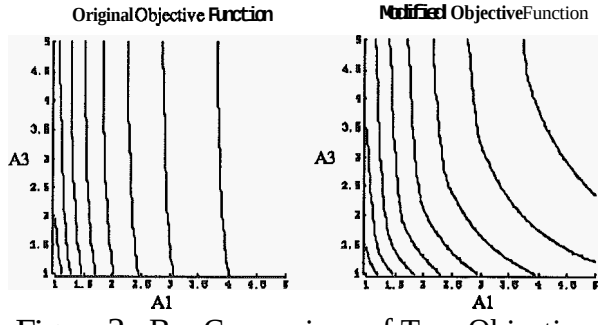

Figure 3 - B Comparison of Two Objective Functions (**A2** = 1.0)

3.5 Shape and Topology Optimization Solution

Figure **4** shows the design domain, the loading conditions and the boundary condition. All loads, material constants and geometrical **data** are the same as the ones in above. The upper limit of the total volume is specified to be 20% of the initial one. Figure **5** shows the optimal material distribution in the design domain obtained by the shape and topology optimization method introduced here. Scale bar indicates material density in each element.

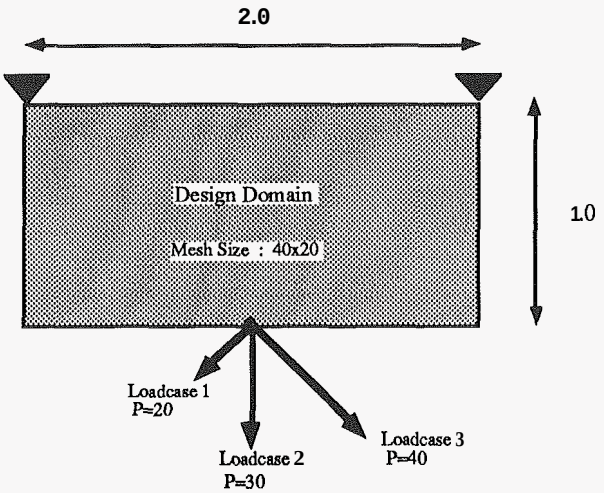

Figure 4 Design Domain with three different loads

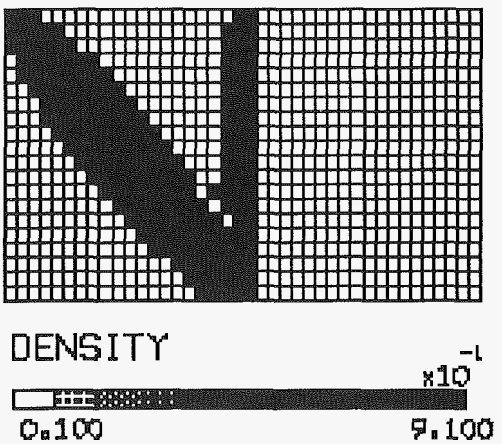

Figure 5 Configuration of Optimal Material Distribution in The Domain

3.6 Discussion

The configuration obtained by the shape and topology optimization method is very similar to the mathematical programming solution using the beam model. One of the reason of difference is that there is no drilling degree of freedom in plate element. Figure 6 shows the material rotational angle distribution in the final configuration. Orientation angles in each load case are continuous and these angles are the same as the directions of the bars. **As** the figure shows, the load case number which is chosen in each element in the formulation of the objective function is almost the same as the mathematical programming solution.

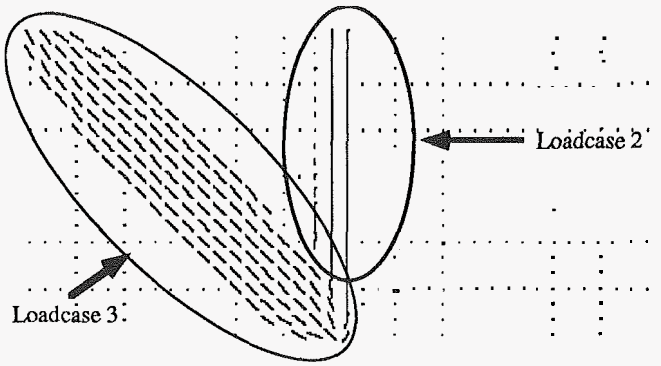

Figure **6** Material Orientation Angle Distribution in Final Configuration

4. Application to Car Body

Examples discussed here are extended to find the optimum layout of a car body with multi loading condition.

4.1 Frame Layout

Figure 7 shows a finite element model and the design domain to simulate a floor reinforcement panel. In plane and out-of-plane loads are applied to the tip of the three dimensional shell model.

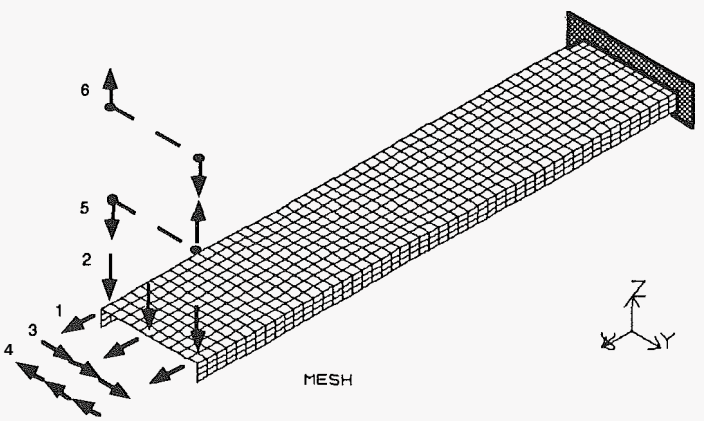

Figure 7 Design Domain for Floor Panel

Figure **8** is the configuration of optimal layout of material distribution in the domain under the volume constraint 60% of initial value. This result shows that some amount of volume can be reduced by putting several holes on the panel.

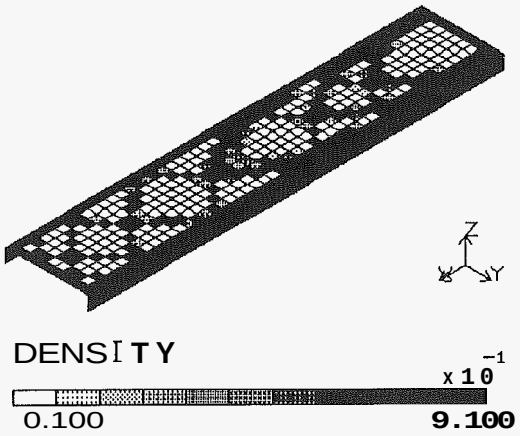

Figure 8 Configuration of Material Distribution in the Domain

4.2 Stiffener Layout on Three Dimensional Shells

Figure 9 shows a finite element model of an automobile engine hood and the design domain. Uniformly distributed and partly distributed loads are applied on the shell as shown in Figure 10.

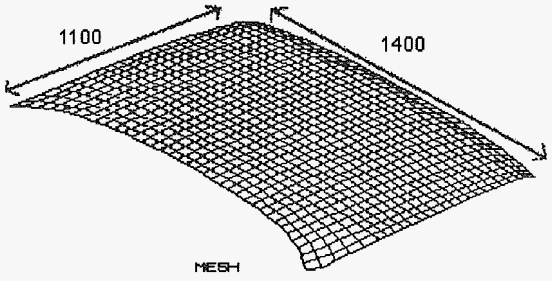

Figure 9 Design Domain for Automobile Engine Hood

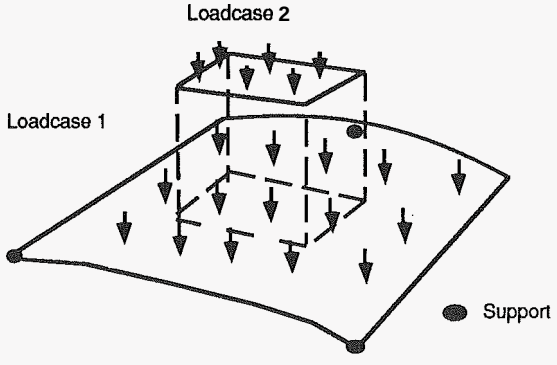

Pressure - Loadcase1 :Loadcase2 = 1 : 2

Figure 10 Loading and Support Condition for the Domain

Figure 11 shows the layout solution by the topology optimization. Ribs are effectively distributed on the shell, and x-shape structure is basically the same as the actual engine hood structure. This result is a little bit unsymmetric because of the difference of material coordinate system defined in each finite element due to the node numbering order.

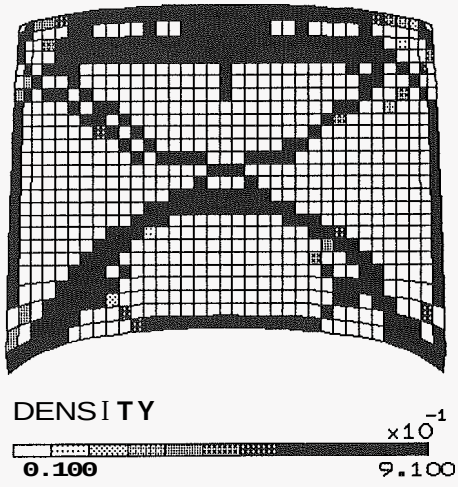

Figure 11 Configuration of The Stiffener Distribution in The Domain

Figure 12 shows the finite element model, loading conditions, support condition, and the design domain for another type of engine hood. Optimal stiffener layout is obtained as shown in figure 13

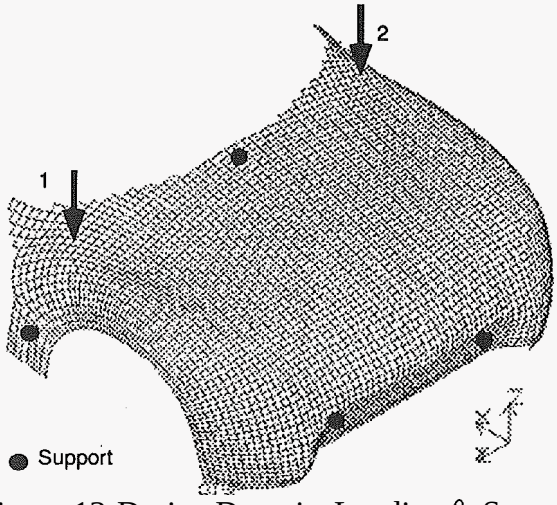

Figure 12 Design Domain, Loading & Support Conditions for Engine Hood II

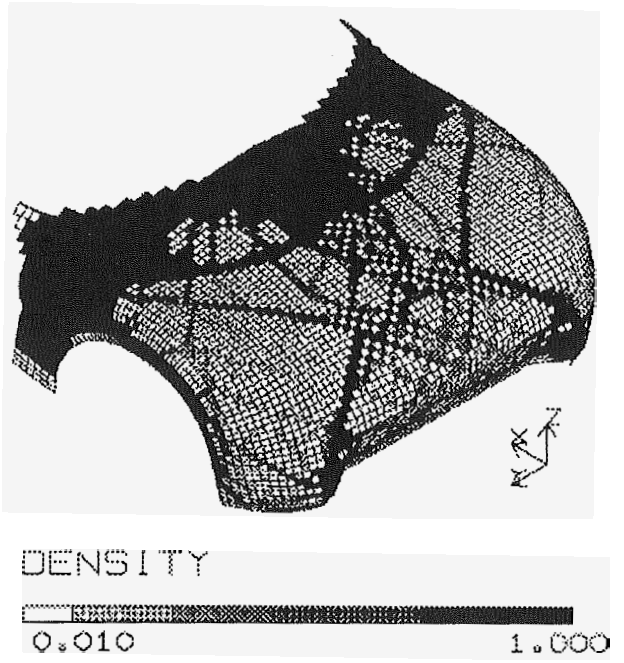

Figure 13 Configuration of The Stiffener Distribution in The Domain

The last example is a stiffener layout of the press door panel. The design domain, loading & support' conditions are shown in figure 14. This type of door is made by stamping and reinforcements may be necessary.

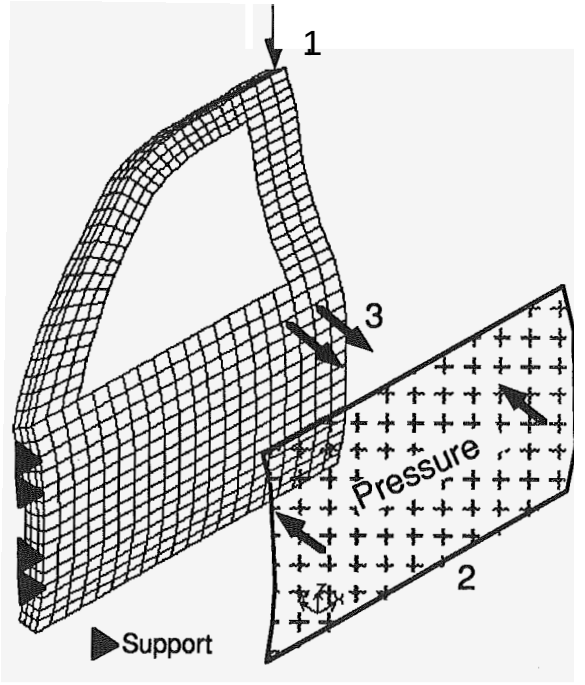

Figure 14 Design Domain, Loading & Support Conditions for Door Panel

Figure 15 is the optimal configuration of stiffener layout on the panel.

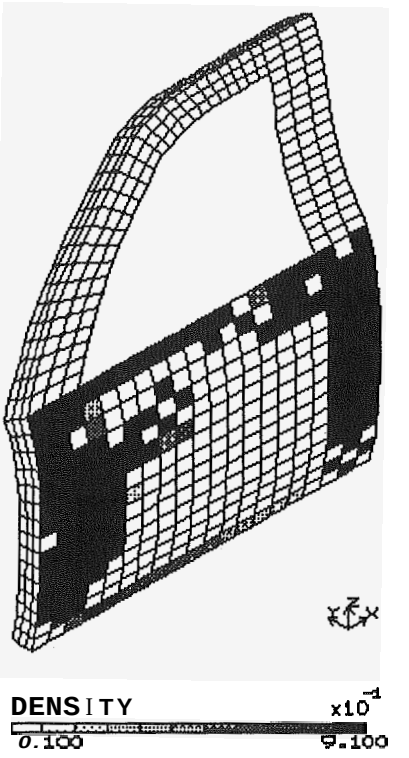

Figure 15 Optimal Stiffener Layout for Door Panel

5. Conclusion

A shape and topology optimization method for multiple loads is given in this paper. This is applicable to actual design problems in automobile design such as frame and stiffener layout problems of a car body. Although our modification of the objective function may not be the best, it can provide physically sound suboptimum solutions with simple optimization algoruthm. Convergence of the algorithm is very stable. It is also noted that Diaz and Bendsøe [9] worked the multi-loading problem using the concept of linear combination without introducing approximation.

6. References

[1] M.P.Bendsøe and N. Kikuchi, "Generating Optimal Topologies in Structural Design using a Homogenization Method," Computer Methods in Applied Mechanics and Engineering, Vol.7 1, 1988, pp 197-224

[2] K.Suzuki and N.Kikuchi, "Homogenization Method for Shape and Topology Optimization," Computer Methods in Applied Mechanics and Engineering.
(to appear)

[3] K.Suzuki, "Shape and Layout Optimization using Homogenization Method,"
PhD dissertation, University of Michigan (1991)

[4] A.Chattopadhyay, J.L.Walsh, and M.F.Riley, "Integrated Aerodynamic/Dynamic Optimization of Helicopter Blades," Proc. AIAA/ASME /-ASCE/AHS 30th Structures,Structural Dynamics and Material Conference, Mobile,Alabama, April 3-5, 1989

[5] J.E.Taylor, Class Note, Dept. of Aerospace Engineering, The University of Michigan, (1990), Ann Arbor, MI

[6] J.Sobieski, A.Dovi, and G Wrenn, "A New Algorithm for General Multiobjective Optimization," NASA TM - 100536, March, 1988

[7] L.A.Schmit and C.Y.Sheu , "Minimum Weight Design of Elastic Redundant Trusses under Multiple Static Loading Conditions", AIAA Journal, Vol. 10, No. 2, pp. 155-162, 1972

[8] G.N.Vanderplaats, DOT User's Manual, Version 2.04, VMA Engineering, Goleta, CA

[9] A.Diaz and M.P.Bendsøe, "Shape Optimization of Multipurpose Structures by a Homogenization Method, Technical Report , Computational Design Laboratory, Michigan State University, (1990), East Lansing, MI

Acknowledgment

The authors would like to thank Mr.Kobayashi and Mr.Kato with Toyota System Research, Inc. The assistance in getting example data is greatly acknowledged.